2009

Re-entrant ferromagnet PrMn2Ge0.8Si1.2: Magnetocaloric effect

S X. Dou
University of Wollongong, shi@uow.edu.au

Jianli Wang
University of Wollongong, jianli@uow.edu.au

Rong Zeng
University of Wollongong, rzeng@uow.edu.au

Chung-Kiak Poh
University of Wollongong, ckp600@uow.edu.au

Stewart J. Campbell
UNSW, stewart.campbell@adfa.edu.au

See next page for additional authors

Re-entrant Ferromagnet $PrMn_2Ge_{0.8}Si_{1.2}$ - Magnetic Properties and Magnetocaloric Effect

J.L. Wang[a,b], S.J. Campbell[a], R. Zeng[c], C.K. Poh[c], S.X. Dou[c] and S.J. Kennedy[b]

[a]School of Physical, Environmental and Mathematical Sciences, The University of New South Wales, The Australian Defence Force Academy, Canberra ACT 2600

[b]Bragg Institute, ANSTO, Menai, NSW 2234

[c]Institute for Superconductivity and Electronic Materials, University of Wollongong, Wollongong, NSW-2522

The structural and magnetic properties of the re-entrant ferromagnet $PrMn_2Ge_{0.8}Si_{1.2}$ have been investigated using x-ray diffraction, magnetic and DSC measurements. Similar to the canonical re-entrant ferromagnet $SmMn_2Ge_2$, multiple magnetic phase transitions have been detected in $PrMn_2Ge_{0.8}Si_{1.2}$ over the temperature range 10 K to 550 K with re-entrant ferromagnetism occurring around ~ 54 K. The magnetocaloric effect has been measured in terms of the isothermal magnetocaloric entropy change and found to be positive at the re-entrant ferromagnetic transition with a maximum value of around 1.9 J/kg K at 58 K for a magnetic field change of 0 to 3 T. On the other hand the entropy change becomes negative (~ -0.5 J/kg K) at the antiferromagnetic to ferromagnetic transition for the same field change. The nature and order of the magnetic transitions have been investigated in detail by means of Arrott plots.

PACS: 75.30.Sg, 75.30.Kz, 71.20.Eh,

Key words: Magnetocaloric effect, Magnetic transitions, Rare earth metals and alloys

Introduction

Investigations of the magnetocaloric effect (MCE) have attracted a great deal of attention [1-3] since Gschneidner and Pecharsky [1] reported an extremely large magnetic entropy change in $Gd_5(Si_2Ge_2)$ close to room temperature, thus offering scope for room temperature magneto-refrigeration. This in turn has led to exploration of a range of materials with potential for large MCE including rare earth elements, rare earth transition metals alloys and manganites [e.g. 2, 3].

Based on mean field theory, both the isothermal magnetic entropy change $\Delta S_M(T)$ and the adiabatic temperature change $\Delta T_{ad}(T)$ are proportional to the derivative of the magnetization with respect to temperature at constant magnetic field [2]. Materials with first order magnetic transitions are therefore of particular interest as they can be expected to exhibit significant MCE at the magnetic transition temperature [2]. In fact, a few compounds showing field-induced magnetic transitions and/or structural transitions [1, 2] have been found to exhibit giant MCE, including $Gd_5(Si_{1-x}Ge_x)_4$, $LaFe_{13-x}M_x$ and $MnFeP_{1-x}As_x$.

As is well known, in RMn_2Ge_2-type compounds the magnetic states and types of magnetic transition and order are highly sensitive to d^a_{Mn-Mn}, the Mn-Mn separation distance in the ab-plane [4]. This type of system therefore offers scope for design of critical magnetic parameters – such as the type or order of magnetic phase transitions and ability to shift transition temperatures - by controlling d^a_{Mn-Mn} with applied or chemical pressure (via substitution with elements of different atomic sizes).

Based on the smaller atomic radius of Si (1.32 Å) compared with Ge (1.37 Å), substitution of Si for Ge in $PrMn_2Ge_2$ leads to a significant decrease in d^a_{MnMn} and a corresponding drastic modification of magnetic states [5]. Here, we outline the influence of substituting Ge with Si in $PrMn_2Ge_{2-x}Si_x$

(x=0.4, 1.0, 1.2 and 1.6) while focusing on the magnetic properties of the re-entrant ferromagnet $PrMn_2Ge_{0.8}Si_{1.2}$ and its magnetocaloric effect at the magnetic transitions.

Experimental

The $PrMn_2Ge_{2-x}Si_x$ alloys with x=0.4, 1.0, 1.2 and 1.6 were prepared by arc melting (five times to aid homogeneity of the ingot) followed by vacuum sealing in a quartz tube and annealing at 1000ºC for a week. In order to compensate for possible loss of Mn during the arc-melting and annealing processes, 3% excess of Mn was added to the initial charges. Room temperature X-ray diffraction (Cu-Kα radiation) was used to check the phase compositions and crystal structures, with the magnetic behavior and transitions investigated by SQUID (5-340 K) and DSC (300-600 K) measurements. The magnetocaloric behavior of $PrMn_2Ge_{0.8}Si_{1.2}$ was determined from M-B curves at selected temperatures.

Results and Discussion

The X-ray diffraction patterns indicate that all samples are single phase and crystallize, as expected, in the $ThCr_2Si_2$ structure (space group I4/mmm). Rietveld refinements of the X-ray diffraction patterns were carried out using the fullprof software and it was found that the lattice parameters decrease as the Si concentration increases [5] with the change in unit cell volume for $PrMn_2Ge_{2-x}Si_x$ given by $dV/dx \sim -7.34$ Å^3. Compared with $PrMn_2Ge_2$, the unit cell volume for $PrMn_2Ge_{2-x}Si_x$ with x=0.4, 1.0, 1.2 and 1.6 has contracted by ~1.4, 3.2, 4.5 and 6.1%, respectively. If we assume that this unit-cell contraction caused by replacement of 60% of the Ge atoms with the smaller Si atoms is equivalent to the effect of applied external pressure, a corresponding pressure of 41.8 kbar can be derived (based on the bulk modulus, B_0=819 kbar, and its pressure derivative, B_0'=4, for $LaMn_2Si_2$ [6]).

The temperature dependence of the magnetization (B=100 Oe; 5-340 K) and DSC results (300-600 K) are shown as a composite figure in Fig. 1. Four magnetic transitions can be identified with the transition temperatures marked by arrows T_1, T_2, T_3 and T_4. Based on the analogous magnetic behavior between $PrMn_2Ge_{0.8}Si_{1.2}$ and other re-entrant ferromagnets such as $SmMn_2Ge_2$ [7], $PrMn_{1.4}Fe_{0.6}Mn_2Ge_2$ [8], $Nd_{0.35}La_{0.65}Mn_2Si_2$ [9], and $NdMn_{1.575}Fe_{0.425}Ge_2$ [10], it is reasonable to ascribe these four transition temperatures T_1, T_2, T_3 and T_4 to be T_C^{Pr}, T_N^{inter}, T_C^{inter} and T_N^{intra}, respectively (the notation used to describe the magnetic structure types and critical transition temperatures is defined in [9]). With decreasing temperature, $PrMn_2Ge_{0.8}Si_{1.2}$ first exhibits a transition from paramagnetism (PM) to an *a–b* plane antiferromagnetic state (AFl) at around T_N^{intra} ~ 435 K. This planar antiferromagnetism then gives way to a *c*-axis ferromagnetic state (Fmc) at around T_C^{inter} ~ 303 K. With further decrease in temperature, a canted antiferromagnetic state (AFmc) is formed at around T_N^{inter} ~ 178 K and, finally, there is a transition to an Fmc state plus ferromagnetic ordering of the Pr sublattice (Fmc+F(Pr)) at T_C^{Pr} ~ 54 K. Confirmation of the magnetic regions and structures identified in Fig 1 and the corresponding magnetic transitions has been obtained from our recent neutron diffraction investigation of $PrMn_2Ge_{2-x}Si_x$ (BENSC, Helmholtz Centre Berlin). As indicated in Fig 1, the main phases in the temperature regions between T_1 and T_2 and between T_2 and T_3 are AFmc and Fmc, respectively. However, it should be noted that the neutron diffraction studies reveal co-existence of the Fmc and AFmc phases in these temperature ranges. As examples, in the AFmc region between T_1 and T_2, 62% AFmc and 38% Fmc are found to co-exist at 140 K while in the Fmc region between T_2 and T_3, 61% Fmc and 39% AFmc are found to co-exist at 240 K. Full details of this neutron investigation will be published elsewhere [11].

As is evident in the insert of Fig. 1 (graphs of dM/dT versus T; B=0.01 T), the transition temperatures T_C^{Pr} and T_N^{inter} reveal hysteresis of about 6 K between the cooling (C) and warming

(W) curves. Compared with the transition temperatures on cooling - T_C^{Pr}(C) ~ 54 K and T_N^{inter}(C) ~ 178 K - on warming the transitions shift to the higher temperatures of T_C^{Pr}(W) ~ 60 K and T_N^{inter}(W) ~ 184 K respectively. As confirmed by our analyses using Arrott plots described below, these temperature hysteretic differences between T_C^{Pr} (C) and T_C^{Pr}(W), and T_N^{inter}(C) and T_N^{inter}(W), indicate that these two transitions are of first order.

The room temperature value of $d^a_{Mn\text{-}Mn}$ for $PrMn_2Ge_{0.8}Si_{1.2}$ is $d^a_{Mn\text{-}Mn}$~2.879 Å: this is similar to the value for $Nd_{0.35}La_{0.65}Mn_2Si_2$ ($d^a_{Mn\text{-}Mn}$~2.878 Å, [9]) but smaller than those for $NdMn_{1.575}Fe_{0.425}Ge_2$ ($d^a_{Mn\text{-}Mn}$~2.886 Å, [10]) and $PrMn_{1.4}Fe_{0.6}Mn_2Ge_2$ ($d^a_{Mn\text{-}Mn}$~2.891 Å, [8]), and larger than the value for $SmMn_2Ge_2$ ($d^a_{Mn\text{-}Mn}$~2.860 Å, 7]). Combined with the fact that this type of re-entrant ferromagnetism does not appear fully in some systems which have similar lattice constants (such as $PrMn_{2-x}Co_xGe_2$ and $NdMn_{2-x}Co_xGe_2$ [12]), we conclude: firstly that the occurrence of re-entrant ferromagnetism in RMn_2Ge_2-based systems is not determined solely by geometric criteria and; secondly, even when re-entrant ferromagnetism occurs in this type of system, the critical distance $d^a_{Mn\text{-}Mn}$ can vary significantly from system to system. Here, we attempt to separate the influences of geometric and electronic factors (due to Si substitution for Ge) on the magnetic transition temperatures in $PrMn_2Ge_{0.8}Si_{1.2}$. Using the known values of T_C^{inter}= 330 K and dT_C^{inter}/dP= - 0.2 K/kbar [13] for $PrMn_2Ge_2$, the calculated value for T_C^{inter} of $PrMn_2Ge_{0.8}Si_{1.2}$ based solely on geometric factors is T_C^{inter}(calc) = 321.6 K. By comparison, the experimental value of T_C^{inter} ~ 303 K (Fig 1) shows a significantly larger decrease of T_C^{inter} than expected due to geometric (chemical pressure effects) alone, thus indicating that the electronic structure differences between Si and Ge also play a critical role in modifying the magnetic states.

Isothermal magnetization curves were recorded over the temperature range 10–340 K in magnetic fields from 0-5.0 T. Typical M-B curves are shown in Fig. 2 for the magnetic regions of interest:

Fig. 2(a) magnetization around T_C^{Pr}; Fig. 2(c) magnetization around T_N^{inter}, and Fig. 2(e) magnetization around T_C^{inter} with the corresponding Arrott Plots of M^2 versus B/M shown in Fig. 3(b), Fig. 2(d) and Fig. 2(f) respectively. The field dependence of the magnetization isotherms obtained at temperatures below T_C^{Pr} and between T_N^{inter} and T_C^{inter} (Figs 2(a), (c), (e)) are found to show FM behavior as expected; this ferromagnetic behavior is confirmed by the positive intercept on the M^2 axis extrapolated from the high fields in the corresponding Arrott plots (Figs 2(b), (d), (f)). By comparison, as these Arrott plots also show, the intercept on the M^2 axis extrapolated from high fields is negative for all temperatures between T_C^{Pr} and T_N^{inter}, and above T_C^{inter}; these findings confirm the antiferromagnetic character of $PrMn_2Ge_{0.8}Si_{1.2}$ over these temperature regions as indicated in Fig 1.

It also can be seen from Fig. 2 that a metamagnetic AF to FM transition with slight magnetic hysteresis is observed (e.g. 90 K and 100 K curves). The Arrott Plot method has been successfully used as a direct and useful tool for distinguishing first-order magnetic transitions from second order magnetic transitions [3]. A positive or negative slope in the isotherm plots of M^2 versus B/M indicates the second-order or first-order character of the transition respectively. For example, the negative slope of the Arrott Plot at 100 K in Fig. 2 (d), indicates the first-order nature of this metamagnetic phase transition from an AF state to a FM state. By comparison, the positive slopes of the Arrott plots above T_C^{inter} as shown in Fig. 2(f) are consistent with a second-order magnetic transition.

The critical fields B_{cr} for the metamagnetic AF to FM transition have been obtained in the standard way from the extreme values of dM/dB in graphs of dM/dB versus B (a typical example at 100 K is shown in the insert of Fig. 3). The temperature dependence of the critical fields in the regions around T_C^{Pr} and T_N^{inter} (Fig. 3) clearly show that the closer to the transition temperature (here T_C^{Pr}

and T_N^{inter}), the smaller the magnetic field needed to induce the metamagnetic transiton from AF to FM. For example, at 65 K, close to the T_C^{Pr} transition and at 160 K (close to T_N^{inter}), a field of B_{cr}=1.1 T is required whereas at 100 K a field of ~2.4 T is required to induce the metamagnetic transition. Moreover, it is clear that an applied magnetic field stabilizes the ferromagnetic state rather than the antiferromagnetism state [8].

The isothermal entropy change, corresponding to a magnetic field change ΔB starting from a zero field to B, has been derived from the magnetization data from the following expression [1]:

$$\Delta S_M(T,B) = \int_0^B \left(\frac{\partial M}{\partial T}\right)_B dB \qquad (1)$$

The change in magnetic entropy change of $PrMn_2Ge_{0.8}Ge_{1.2}$ as a function of temperature as derived from Eq. 1 is shown in Fig. 4(a). The curves of $-\Delta S_M$ versus T provide valuable information about the nature of the magnetic transitions in $PrMn_2Ge_{0.8}Ge_{1.2}$ Around the region of the T_N^{inter} transition, $T_N^{inter} \approx 178$ K, $-\Delta S_M$ is negative (thus indicating an inverse MCE); this corresponds to the magnetic transition from the lower-temperature AFmc phase of lower magnetic moment (e.g. M_s=0 Am^2/kg at 160 K) compared to the higher-temperature Fmc phase of larger magnetic moment (e.g. M_s=23.8 Am^2/kg at 190 K) (Fig. 1). By comparison positive values of $-\Delta S_M$ are detected at both T_C^{Pr} (from Fmc+F(Pr) to AFmc) and T_C^{inter} (from Fmc to AFl) with this behaviour related to transitions from a lower-temperature state of larger magnetic moment to a higher-temperature, lower moment state (e.g. M_s=26.8 Am^2/kg at 50 K while M_s=0 Am^2/kg at 60 K and 24.8 Am^2/kg at 290 K while M_s=0 Am^2/kg at 310 K, respectively). The maximum value of $-\Delta S_M$ is ~ 2.6 J/kg K at 58 K for a magnetic field change of 0 to 5 T with $-\Delta S_M$ values of ~ -0.6 J/kg K and ~ 2.2 J/kg K at 150 K and 315 K for the same field change, respectively.

Fig. 4(b) shows a graph of $-\Delta S_M$ plotted as a function of $(B/T)^{2/3}$ for data in the region around the three transition temperatures T_C^{Pr}, T_N^{inter} and T_C^{inter}. Mean field theory predicts that $-\Delta S_M$ is proportional to $(B/T)^{2/3}$ at second order phase transitions [14]. The linear fits to the data in Fig. 4(b) demonstrate that the relationship $-\Delta S_M \propto (B/T)^{2/3}$ is valid around T_C^{inter} (adjusted R square is 0.9997) but that the field dependence of the maximum entropy change deviates from linear behaviour in $(B/T)^{2/3}$ at both T_C^{Pr} (adjusted R square is 0.997) and T_N^{inter} (adjusted R square is 0.897) where first order transitions occur.

In conclusion, Si substitution for Ge in $PrMn_2Ge_2$ leads to a modification of the magnetic state which can not be ascribed solely to geometric factors but also results from differences in the electronic structures of Ge and Si. The nature and order of the magnetic transitions as well as the magnetocaloric effect have been investigated in detail by DC magnetic measurements. Both conventional and inverse magnetocaloric effects have been observed in polycrystalline samples of the re-entrant ferromagnet $PrMn_2Ge_{0.8}Si_{1.2}$ (Fig 4(a)) indicating that materials which exhibit re-entrant ferromagnetism can offer a route towards acceptable magnetocaloric effects.

References

[1] V. K. Pecharsky and K. A. Gschneidner, Jr., Phys. Rev. Lett. **78**, 4494 (1997)

[2] E. Brück, J. Phys. D: Appl. Phys. **38,** R381 (2005); O. Tegus, E. Brück, K. H. J. Buschow, and F. R. de Boer, Nature (London) **415**, 150 (2002)

[3] K. A. Gschneidner, V.K. Pecharsky and A.O. Tsokol, Rep. Prog. Phys. **68**, 1479 (2005)

[4] A. Szytula, J. Leciejewicz, Handbook of Crystal Structures and Magnetic Properties of Rare Earth Intermetallics, CRC Press, Boca Raton, 1994

[5] S Kervan, A Kilic and A Gencer, J. Phys.: Condens. Matter **16,** 4955 (2004)

[6] M. Hofmann, S.J. Campbell, K. Knorr, S. Hull and V. Ksenofontov, J. Appl. Phys. **91**, 8126 (2002)

[7] G.J. Tomka, C. Ritter, P.C. Riedi, Cz. Kapusta and W. Kocemba Phys. Rev. B **58,** 6330 (1998)

[8] J.L. Wang, S.J. Campbell, J.M. Cadogan, O. Tegus, A J Studer and M Hofmann, J. Phys.: Condens. Matter **18**, 189 (2006); I. Dincer, A. Elmali, Y. Elerman, H. Ehrenberg, H. Fuess and G. Andre, J. Alloy. Comp. **416,** 22 (2006)

[9] G. Venturini, R. Welter, E. Ressouche and B. Malaman, J. Magn. Magn. Mater. **150** 197 (1995)

[10] G. Venturini, B. Malaman and E. Ressouche, J. Alloy. Comp. **237,** 61 (1996)

[11] J.L. Wang, S.J. Campbell, M. Hofmann *et al.* "Neutron Diffraction Study of Magnetic Phases in $PrMn_2Ge_{2-x}Si_x$" (in preparation, 2008).

[12] I. Dincer, Y. Elerman, A. Elmali, H. Ehrenberg and H. Fuess, J. Alloy. Comp. **334,** 72 (2002)

[12] T. Kawashima, T. Kanomata, H. Yoshida and T. Kaneko, J. Magn. Magn. Mater. **90-91**, 721 (1990)

[14] H. Oesterreicher and F. T. Parker, J. Appl. Phys. **55**, 4334 (1984)

Figure captions

Fig. 1 (color online) Composite figure showing the temperature dependent magnetization obtained on cooling $PrMn_2Ge_{0.8}Si_{1.2}$ in a field of B=0.01 T (left part) and the DSC results (right part). The insert shows the dM/dT versus T plots for both warming and then cooling after first cooling from room temperature in zero field (transition temperatures indicated by arrows). As discussed in the text, the four transition temperatures T_1, T_2, T_3 and T_4 are linked with the ordering transitions T_C^{Pr}, T_N^{inter}, T_C^{inter} and T_N^{intra} respectively.

Fig. 2 (color online) (a), (c) and (e) Field dependence of magnetization of $PrMn_2Ge_{0.8}Si_{1.2}$ at the temperatures around T_C^{Pr}, T_N^{inter} and T_C^{inter} as indicated (see text) and

(b), (d) and (f) the corresponding Arrott plots (M^2 versus B/M).

Fig. 3 (color online) Temperature dependence of the critical magnetic field, B_{cr}, of the metamagnetic transition. As discussed in the text, the insert shows the dM/dB versus B curve at T = 100 K as a typical example of how B_{cr} is determined.

Fig. 4 (color online) (a) Temperature dependence of the isothermal magnetic entropy change $-\Delta S_M$ *(T, B)* and (b) dependence of the entropy changes on $(B/T)^{2/3}$. The linear fits to the data around the three magnetic phase transition temperatures: T_c^{Pr}, T_N^{inter} and T_C^{inter} are described in the text.

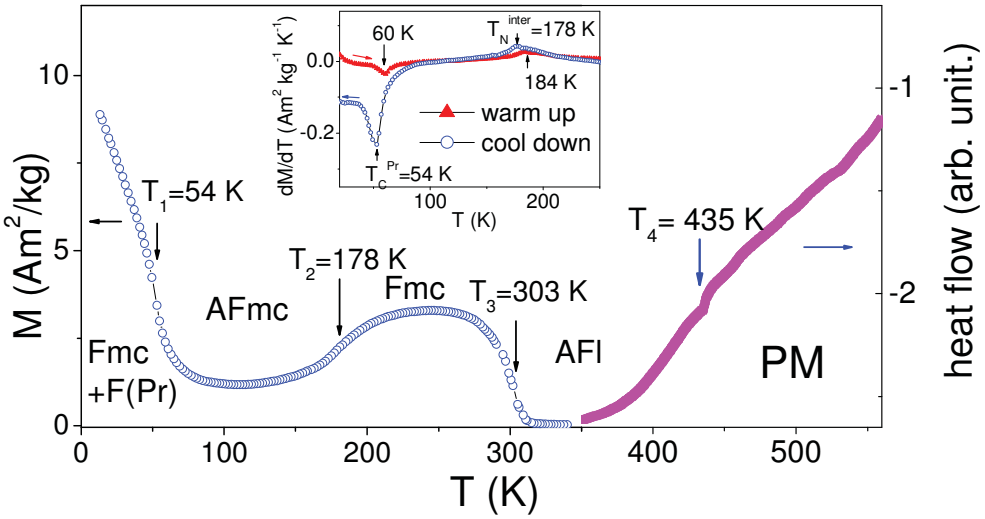
M (Am²/kg)
T (K)
heat flow (arb. unit.)
T1=54 K
T2=178 K
T3=303 K
T4= 435 K
Fmc
+F(Pr)
AFmc
Fmc
AFI
PM
60 K
T_N^inter=178 K
184 K
T_C^Pr=54 K
warm up
cool down
dM/dT (Am² kg⁻¹ K⁻¹)
T (K)

Fig. 1

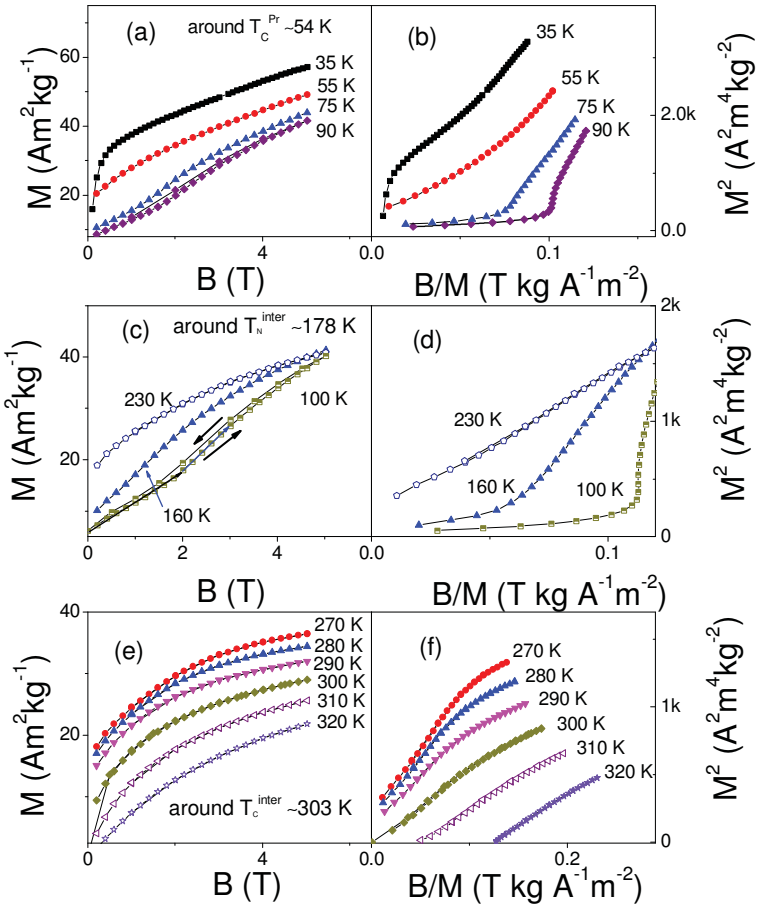
(a)
around T_C^{Pr} ~54 K
35 K
55 K
75 K
90 K
M (Am^2kg^{-1})
B (T)
(b)
35 K
55 K
75 K
90 K
2.0k
0.0
B/M (T kg $A^{-1}m^{-2}$)
M^2 ($A^2m^4kg^{-2}$)
(c)
around T_N^{inter} ~178 K
230 K
100 K
160 K
M (Am^2kg^{-1})
B (T)
(d)
230 K
160 K
100 K
2k
1k
0
B/M (T kg $A^{-1}m^{-2}$)
M^2 ($A^2m^4kg^{-2}$)
(e)
270 K
280 K
290 K
300 K
310 K
320 K
around T_c^{inter} ~303 K
M (Am^2kg^{-1})
B (T)
(f)
270 K
280 K
290 K
300 K
310 K
320 K
1k
0
B/M (T kg $A^{-1}m^{-2}$)
M^2 ($A^2m^4kg^{-2}$)

Fig. 2

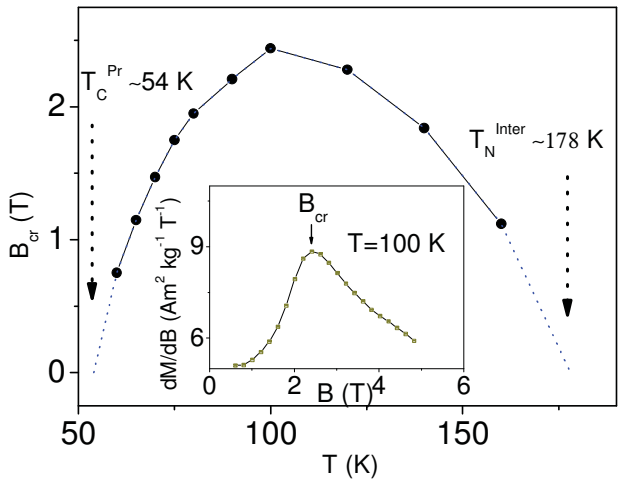

Fig. 3

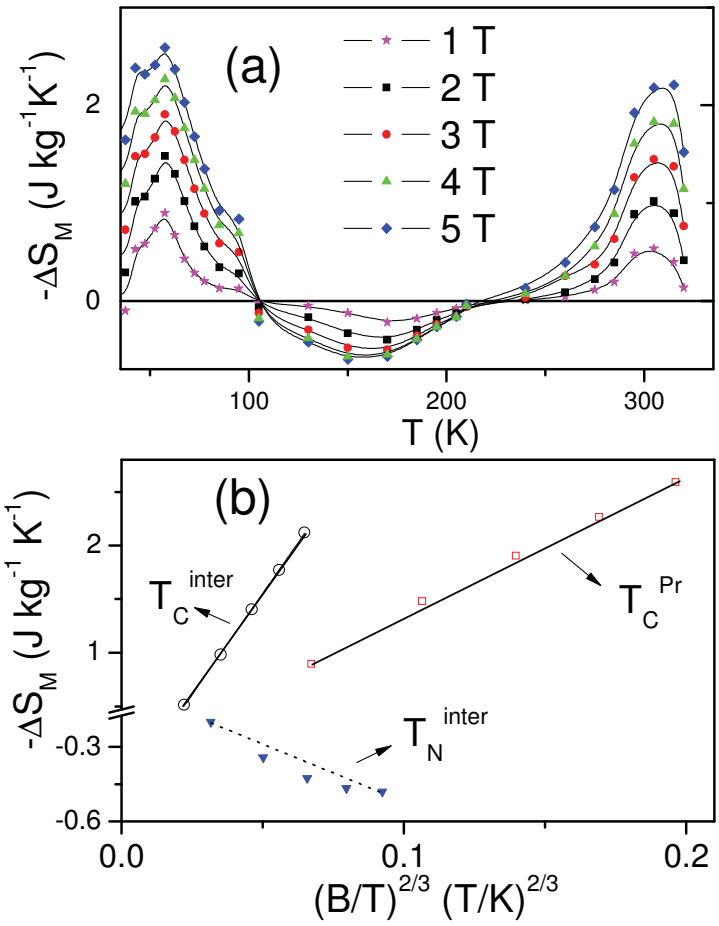
(a)
1 T
2 T
3 T
4 T
5 T
-ΔS_M (J kg^-1 K^-1)
T (K)
(b)
T_C^inter
T_C^Pr
T_N^inter
-ΔS_M (J kg^-1 K^-1)
(B/T)^2/3 (T/K)^2/3

Fig. 4